Department of Energy, under Contract W-31-109-ENG-38 and Grant DE-FG05-86ER45259, respectively. We express our appreciation for computing time on the ER-Cray X-MP computer, made available by DOE. We wish to thank Professor H. Kobayashi for kindly providing coordinates for the κ-$(ET)_2I_3$ salt.

Registry No. κ-$(ET)_2X$ ($X = Cu(NCS)_2^-$), 113132-62-0; κ-$(ET)_2X$ ($X = I_3^-$), 89061-06-3; κ-$(MD)_2AuI_2$, 120389-59-5; κ-$(MT)_2Au(CN)_2$, 110899-47-3.

Contribution from the Department of Chemistry and Laboratory for Molecular Structure and Bonding, Texas A&M University, College Station, Texas 77843

Solid-State Geometric Isomers of $Re_2H_8(PPh_3)_4$

F. Albert Cotton* and Rudy L. Luck

Received June 19, 1989

Complexes of the form $Re_2H_8(PR_3)_4$, PR_3 = tertiary-phosphine ligand, have previously been shown in the solid state to be arranged as $(PR_3)_2H_2Re(\mu\text{-}H)_4ReH_2(PR_3)_2$, with the P atoms attached to the adjacent Re atoms being eclipsed (D_{2h} symmetry). The structure of the complex $Re_2H_8(PPh_3)_4$ in the crystalline state is shown here to depend on the solvents used to grow crystals. A crystal form (**1a**) containing a planar eclipsed arrangement, as found previously, consisting of four P and two Re atoms is obtained if hexane is allowed to diffuse slowly into a tetrahydrofuran (THF) solution of the complex. However, a crystal form (**1b**) containing a staggered arrangement of the four P atoms is obtained if crystals are obtained from a saturated solution of $Re_2H_8(PPh_3)_4$ in acetone. The variable-temperature ^1H NMR spectra of this complex in CD_2Cl_2 are also reported. Crystal data: $Re_2H_8(PPh_3)_4 \cdot 2C_4H_8O$ (**1a**) (THF/hexane): monoclinic, space group $C2/c$, a = 20.592 (9) Å, b = 17.828 (4) Å, c = 18.837 (4) Å, β = 90.97 (3)°, V = 6914 (4) Å^3, Z = 4, R = 0.0469 (R_w = 0.0625) for 321 parameters and 3822 unique data having $F_o^2 > 3\sigma(F_o^2)$. $Re_2H_8(PPh_3)_4 \cdot (CH_3)_2CO$ (**1b**) (acetone): monoclinic, space group $C2/c$, a = 23.414 (5) Å, b = 13.281 (2) Å, c = 23.702 (4) Å, β = 114.84 (2)°, V = 6688.4 (7) Å^3, Z = 4, R = 0.0328 (R_w = 0.0464) for 336 parameters and 4316 unique data having $F_o^2 > 3\sigma(F_o^2)$. **1a** also shows a systematic disordering of 4% of the molecules, from which a possible mechanism (an internal flip of Re_2) for exchange of bridge and terminal hydrogen atoms may be inferred.

Introduction

In 1969 Chatt and Coffey[1] reported two incompletely characterized but extremely interesting compounds, which they tentatively formulated as $[ReH_x(PR_3)_2]_2$. PR_3 was either PEt_2Ph or PPh_3 and x was believed to have a value less than 7. These were called "agnohydrides" because of their uncertain composition and nature. In 1977, Bau et al.[2] reported a neutron diffraction study of the one with PEt_2Ph and showed that it has the composition $Re_2H_8(PEt_2Ph)_4$ and the structure shown schematically in I. In the intervening years, the synthetic procedures[3] for these

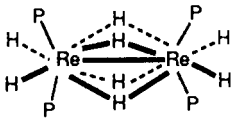

P = PEt_2Ph

I

compounds have been improved, more has been learned about their reaction chemistry,[4-6] and, of particular interest to us, their NMR behavior has been examined.[7] The main features of interest in this last connection are (1) that the bridge and terminal H atoms are rapidly (i.e., on the NMR time scale) undergoing site exchange at room temperature[2,3b,7] and (2) the longitudinal relaxation times (T_1's) for these hydrogen atoms are relatively short at low temperatures.[7]

Two interesting aspects of these compounds that have not received sufficient attention have been structural studies and the question of how the H_t-H_b exchange may be accomplished. In this paper we report structural results on $Re_2H_8(PPh_3)_4$ (one of the two original agnohydrides) as well as some ideas on the manner in which the remarkably facile H_t-H_b exchange may occur.

Table I. Crystallographic Data for $Re_2H_8(PPh_3)_4 \cdot 2C_4H_8O$ (**1a**) and $Re_2H_8(PPh_3)_4 \cdot (CH_3)_2CO$ (**1b**)

	$C_{80}H_{84}O_2P_4Re_2$ (**1a**)	$C_{75}H_{74}OP_4Re_2$ (**1b**)
fw	1577.81	1511.74
a, Å	20.592 (9)	23.414 (5)
b, Å	17.828 (4)	13.281 (2)
c, Å	18.837 (4)	23.702 (4)
β, deg	90.97 (3)	114.84 (2)
V, Å^3	6914 (4)	6688.4 (7)
Z	4	4
space group	$C2/c$ (No. 15)	$C2/c$ (No. 15)
T, °C	+19	-80
λ, Å	0.71073	0.71073
ρ_{calcd}, g/cm^{-3}	1.516	1.501
μ, cm^{-1}	36.806	38.022
transm coeff	100.00-81.74	99.79-55.65
$R(F_o)^a$	0.0469	0.0328
$R_w(F_o)$	0.0625[b]	0.0464[c]

[a] $R = \sum||F_o| - |F_c||/\sum|F_o|$. [b] $R_w = [\sum w(|F_o| - |F_c|)^2/\sum w|F_o|^2]]^{1/2}$; $w = 1.3837/[\sigma^2(|F_o|) + 0.001(F_o^2)]$. [c] $R_w = [\sum w(|F_o| - |F_c|)^2/\sum w|F_o|^2]^{1/2}$; $w = 1.1869/[\sigma^2(|F_o|) + 0.001(F_o^2)]$.

Experimental Section

The NMR spectra were recorded in CD_2Cl_2 by using a Varian XL-400 spectrometer. The complex $Re_2H_8(PPh_3)_4$ was obtained in this study either by following the published procedures[1] as a product of the thermal transformation of $ReH_7(PPh_3)_2$ or as a byproduct (27% yield, verified by ^1H NMR relative to $ReH_5(PPh_3)_3$) in an adaptation of a procedure[8]

(1) Chatt, J.; Coffey, R. S. *J. Chem. Soc. A* **1969**, 1963.
(2) Bau, R.; Carroll, W. E.; Teller, R. G.; Koetzle, T. F. *J. Am. Chem. Soc.* **1977**, *99*, 3872.
(3) (a) Brant, P.; Walton, R. A. *Inorg. Chem.* **1978**, *17*, 2674. (b) Fanwick, P. E.; Root, D. R.; Walton, R. A. *Inorg. Chem.* **1989**, *28*, 395. (c) Roberts, D. A.; Geoffroy, G. L. *J. Organomet. Chem.* **1981**, *214*, 221.
(4) Allison, J. D.; Walton, R. A. *J. Chem. Soc., Chem. Commun.* **1983**, 401.
(5) Moehring, G. A.; Fanwick, P. E.; Walton, R. A. *Inorg. Chem.* **1987**, *26*, 1861.
(6) Allison, J. D.; Cotton, F. A.; Powell, G. L.; Walton, R. A. *Inorg. Chem.* **1984**, *23*, 159.
(7) (a) Cotton, F. A.; Luck, R. L. *Inorg. Chem.* **1989**, *28*, 6. (b) Cotton, F. A.; Luck, R. L.; Root, D. R.; Walton, R. A. *Inorg. Chem.*, in press.
(8) Douglas, P. G.; Shaw, B. L. *Inorg. Synth.* **1977**, *17*, 64.

0020-1669/89/1328-4522$01.50/0

Table II. Variation of R, R_w, and Quality of Fit (QOF) Parameters with Different Refinement Models for Complex **1b**

	no metal-bonded H atoms	metal-bonded H atoms	no metal-bonded H atoms	metal-bonded H atoms
2θ, deg	35	35	50	50
R^a	2.88	2.69	3.36	3.28
R_w^b	4.62	4.21	4.86	4.64
QOF[c]	1.35	1.24	1.22	1.16

[a] $R = \sum||F_o| - |F_c||/\sum|F_o|$. [b] $R_w = [\sum w(|F_o| - |F_c|)^2/\sum w|F_o|^2]^{1/2}$; $w = 1.1869/[\sigma^2(|F_o|) + 0.001(F_o^2)]$ for the last column. [c] QOF = quality of fit $= [\sum w(|F_o| - |F_c|)^2/(N_{observns} - N_{params})]^{1/2}$.

(PPh_3 was used instead of PMe_2Ph) that was intended to produce $ReH_5(PPh_3)_3$ (73% yield).

The crystal of $Re_2H_8(PPh_3)_4$, that revealed the eclipsed from **1a** was obtained from the slow diffusion of hexane into a THF solution of the material obtained in the first procedure outlined above, and contained two C_4H_8O molecules per $Re_2H_8(PPh_3)_4$. The crystals that revealed the geometric isomer form **1b** were obtained by allowing crystallization from a concentrated solution in acetone of the $Re_2H_8(PPh_3)_4$ obtained via the second procedure outlined above, and contained one $(CH_3)_2CO$ per $Re_2H_8(PPh_3)_4$. However, when crystals of either type are dissolved in CD_2Cl_2, the same ^1H NMR spectrum is observed for the $Re_2H_8(PPh_3)_4$ molecule.

Pertinent crystallographic information is given in Table I (and as supplementary material; see paragraph at end of paper regarding supplementary material). In the case of **1a**, a bricklike crystal was coated with epoxy resin and mounted on top of a glass fiber. For **1b**, a suitable crystal was mounted with epoxy on top of a quartz fiber. The X-ray data were collected, the space group $C2/c$ was initially chosen on the basis of the systematic absences, and corrections were made as previously described[9] in both cases. Most of the non-hydrogen atoms comprising a complete molecule were located from a three-dimensional Patterson function in each case. The Re atoms in each structure were located off crystallographic 2-fold axes, which in the case of **1a** was located perpendicular to a plane described by the Re and the two P atoms. For **1b**, discussed below, this crystallographic axis is located perpendicular to the Re–Re bond but rotated clockwise 39° from the planes defined by the two ReP_2 groups.

In the case of **1a**, after these atoms had been refined to convergence anisotropically by using the Enraf-Nonius SDP software[10a,b] a difference map revealed two peaks that could only represent a fractional Re_2 unit in a minor orientation, essentially perpendicular to the first one and in the same plane as the first set of Re and P atoms. Subsequent refinement was performed with the SHELX-76 package of programs.[10c] A model containing both the principal and the secondary rhenium atoms was refined, with the sum of the fractional occupanicies of the two Re atoms constrained to be unity. This resulted in the occupancies given in the footnote of Table II. A subsequent difference map revealed the positions of the two P atoms bonded to the Re atom in the minor orientation. These were refined isotropically. All of the atoms in the principal molecule were refined with occupancies set at 96%. The Re atom and two P atoms in the secondary molecule were refined with occupancies of 4%. Hydrogen atoms were entered, with 96% occupancies, at calculated positions for the phenyl rings. The phenyl groups were then refined as rigid bodies, and the thermal parameters on all of the hydrogen atoms attached to phenyl carbon atoms were constrained to the same value, which was refined. A final difference map revealed two disordered THF molecules around different inversion points. These were refined with constraints set up for the adjacent C–C distances and with all of their thermal parameters constrained to the same value, which was refined. This whole model was then refined to convergence, resulting in the final figures of merit listed in Table I.

For **1b**, the positions of the atoms were also refined to convergence anisotropically by using the Enraf-Nonius SDP software.[10a,b] The difference map at this stage showed no sign of disorder with respect to the Re atom but did reveal quite clearly one ordered acetone molecule in the asymmetric unit. Subsequent refinement was performed with the SHELX-76 package of programs.[10c] Hydrogen atoms were entered at calculated positions for the phenyl rings. This model with the phenyl groups refined as previously described above for those on **1a** was refined to convergence. A difference map at this stage contained peaks of significant electron density that were in likely positions (two terminal per Re atom, two bridging on the 2-fold axis, and one bridging off the 2-fold axis, which generates another by symmetry) for the bridging and terminal hydrides. Insertion of these into the model as hydrogen atoms followed by free refinement led to unrealistic distances and thermal parameters for these metal-bonded hydrogen atoms.

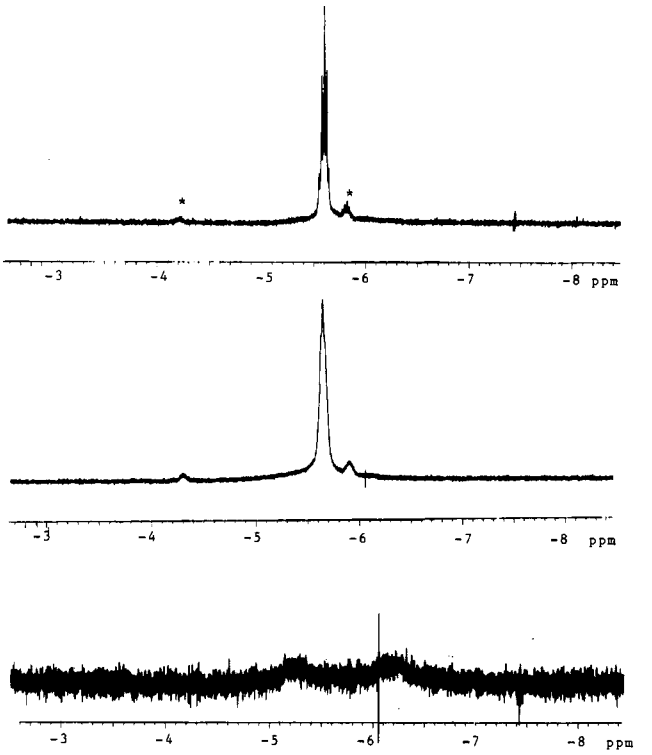

Figure 1. ^1H NMR spectra of $Re_2H_8(PPh_3)_4$ in the hydride region only at 400 MHz in CD_2Cl_2 at temperatures of +22 (top), −60 (middle) and ca. −110 °C (bottom). The precise assignments of the two small multiplets, denoted by asterisks in the spectrum obtained at 22 °C, are not known.

To ascertain if the initially determined positions for these hydrogen atoms were reasonable, two difference Fourier maps were done with the converged model (excluding the metal-bonded hydrogen atoms), first with all of the data (the full difference map) and then only with data up to $(\sin\theta)/\lambda$ of 0.423 (the low-angle difference map). The results were then represented in the form of several contour plots which were submitted as supplementary material (see paragraph at end of paper regarding supplementary material). This type of analysis was established as useful in earlier studies on the location of metal-bonded hydrogen atoms in $H_3Mn_3(CO)_{12}$[11] and $Mo_2(\eta^5\text{-}C_5H_5)_2(CO)_4(\mu\text{-}H)(\mu\text{-}P(CH_3)_2)$.[12]

A comparison between the two sets of contour plots reveals the following points: (1) The peaks ascribed to H atoms in the full difference map are also present in the low-angle map. (2) They occur much higher in the latter map. In fact, they are 3, 4, 5, 6, and 14 in a list of residual peaks in order of decreasing intensity. (3) The two highest peaks in either difference Fourier map are at positions roughly in the middle of the Re–Re bond. It is probably not correct to assign these as due entirely to the bonding electrons of the Re–Re bond as there is no sign of the corresponding negative electron density at the Re atom sites that would be associated with this assignment, but this may account for them at least partly. Similar effects were found and ascribed to the bonding electrons in the case of $Mo_2(O_2CPh)_4$.[13] (4) Finally, there is significant electron density located trans to the Re–Re bond in both directions.

It was decided to use the positions obtained in the low-angle difference map for the metal-bonded hydrogen atoms since these are likely to be the ones most accurately determined in this experiment. The constraints that the terminal d(Re–H) = 1.476 (5) Å and the bridgng d(Re–H) = 1.952 (5) Å and that H(3)–H(4) = 2.04 (5) Å and H(3)–H(5) = 2.18 (5) Å were then applied to these metal-bonded hydrogen atoms by using

(9) Bino, A.; Cotton, F. A.; Fanwick, P. E. *Inorg. Chem.* **1979**, *18*, 3558.
(10) (a) Calculations were done on a Local Area VAX Cluster, employing the VAX/VMS V4.6 computer. (b) Sheldrick, G. M. "SHELXS-86", Institut fur Anorganische Chemie der Universität, Göttingen, FRG, 1986. (c) Sheldrick, G. M. "SHELX-76", University of Cambridge, 1976.
(11) Kirtley, S. W.; Olsen, J. P.; Bau, R. *J. Am. Chem. Soc.* **1973**, *95*, 4532.
(12) Petersen, J. L.; Williams, J. M. *Inorg. Chem.* **1978**, *17*, 1308.
(13) Troup, J. M.; Extine, M. W.; Ziolo, R. F. In *Electron Distribution and the Chemical Bond*; Coppens, P., Hall, M. B., Eds.; Plenum Press: New York, 1982; p 285.

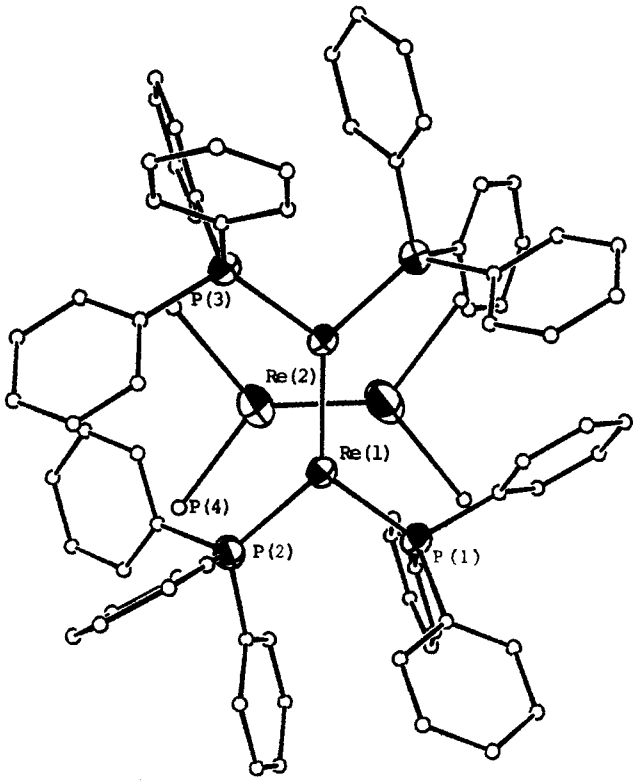

Figure 2. ORTEP drawing of complex **1a** showing the perpendicular arrangement of the Re(2)P(3)P(4) unit in the minor orientation. The ellipsoids represent thermal displacements and are drawn at the 50% probability level. Carbon atoms and the P atoms on the molecule in the minor orientation are represented by circles of arbitrary size.

the DFIX instruction card.[9c] This was done to keep the Re–H distances at a more realistic length. The thermal parameters of these hydrogen atoms were refined freely. This model was then refined to convergence, resulting in the final figures of merit listed in Table I. Some indication of the significance of these peaks as metal-bonded hydrogen atoms is shown in Table II, which lists the R, R_w, and esd parameters for various refinement models. There are appreciable improvements in these figures of merit with the inclusion of the peaks as hydrogen atoms. The fractional atomic coordinates for **1a** and **1b** are located in Tables III and IV, respectively. Selected bond distances and angles are listed in Table V for **1a** and Table VI for **1b**. Table VI also contains selected nonbonded geometric information.

Discussion

NMR Studies. The variable-temperature ^1H NMR spectra, in CD_2Cl_2 and in the hydride region only, of $Re_2H_8(PPh_3)_4$ are presented in Figure 1.[7b] The metal-bonded hydrogen atoms give rise to a quintet at δ −5.6 at room temperature as stated previously.[1,2,7b] This pattern coalesces at −60 °C into a broad peak at δ −5.7, which is resolved into two peaks at δ −5.3 and δ −6.3 at −120 °C as shown in Figure 1.[7b] These two peaks are due to the resonances from the frozen-out bridging and terminal metal-bonded hydrogen atoms. Some ideas as to possible mechanisms of interchange are discussed below.

Crystallographic Results. An ORTEP drawing of **1a** (exclusive of the THF molecules) is presented in Figure 2. Both the principal and secondary molecules are positioned at a center of inversion ($^1/_2$, $^1/_4$, $^1/_4$) so that half of each dimer molecule constitutes the asymmetric unit. Unfortunately, none of the metal-bonded hydrogen atoms were discerned in the final difference map for **1a**.

The two molecules partially occupying the site are essentially perpendicular (calculated angle between Re–Re lines = 89.8 (6)°). The two P_2ReReP_2 units are coplanar within experimental error. The disorder is reminiscent of, but not exactly the same as, that often seen in $M_2X_8^{n-}$ species and their derivatives (see $Re_2I_8^{2-}$ for an example and earlier references[14]). In those cases the entire set of ligand atoms is essentially the same for both M_2 units, whereas here the metal-bonded H atoms and the PPh_3 ligands of the two molecules must be in distinctly different sites.

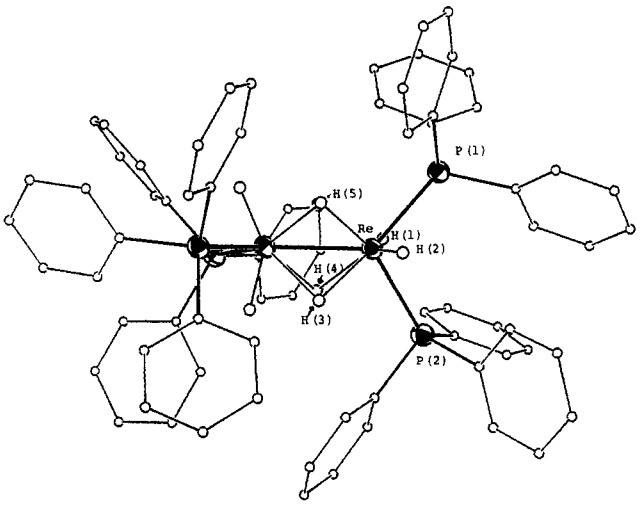

Figure 3. ORTEP drawing of complex **1b**. The ellipsoids and circles (used in this drawing to depict the metal-bonded hydrogen atoms also) are drawn as in Figure 1.

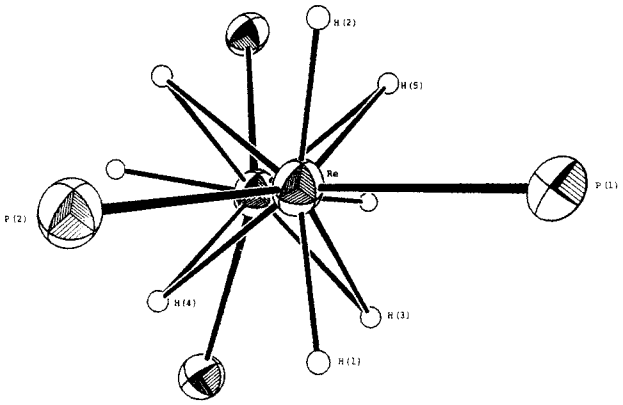

Figure 4. ORTEP drawing of complex **1b** drawn almost perpendicular to the Re–Re bond with the ellipsoids and spheres as in Figure 3. Carbon atoms on the phenyl rings have been omitted for clarity.

An ORTEP drawing of the $Re_2H_8(PPh_3)_4$ molecule in **1b** is presented in Figure 3. A different of view of this molecule without the phenyl groups on the PPh_3 ligand, looking approximately down the Re–Re bond, is shown in Figure 4. This shows quite clearly the staggered arrangement of the two ReP_2 units. The structure approximates to, but is definitely distorted from, an idealized D_{2d} symmetry. The angle between the two ReP_2 planes along the Re–Re axis is 77.6°. The arrangement of the metal-bonded H atoms, deduced and refined with the distances determined from data up to $(\sin\theta)/\lambda = 0.423$, is also depicted in this drawing. The terminal metal-bonded H atoms on one Re atom occupy sites eclipsing the P atoms on the other Re atom, and the bridging hydrogen atoms occupy positions that are roughly staggered with respect to the terminally bonded H and P atoms. The determination of the metal-bonded H atoms is important, for it confirms the stoichiometry of the product as $Re_2H_8(PPh_3)_4$ as opposed to the possibility that the geometry of **1b** is due to the presence of a different number of bridging H atoms. Although the exact distances for these metal-bonded H atoms were not determined accurately, it is clear that complex **1b** is not exactly staggered with respect to the arrangements of the two ReP_2 groups that constitute the molecule.

It has been suggested[15] that the rotation of a terminal group in the complex $Re_2H_8(PH_3)_4$ is a very facile process and that there

(14) Cotton, F. A.; Daniels, L. M.; Vidyasagar, K. *Polyhedron* **1988**, *7*, 1667.

(15) Dedieu, A.; Albright, T. A.; Hoffmann, R. *J. Am. Chem. Soc.* **1979**, *101*, 3141.

Table III. Positional Parameters and Their Estimated Standard Deviations for $Re_2H_8(PPh_3)_4 \cdot 2C_4H_8O$ (**1a**)[a]

atom[b]	x	y	z	B, Å²
Re(1)	0.43863 (2)	0.26328 (2)	0.25350 (2)	2.660 (9)
P(1)	0.3637 (1)	0.2646 (2)	0.1576 (1)	2.85 (6)
P(2)	0.3715 (1)	0.2612 (2)	0.3534 (1)	2.91 (6)
Re(2)	−0.0047 (6)	0.2457 (8)	0.6832 (7)	5.8 (4)
P(3)	0.395 (2)	0.259 (3)	0.104 (3)	1 (1)*
P(4)	0.417 (3)	0.253 (3)	0.401 (4)	4 (1)*
C(111)	0.3121 (3)	0.1819 (4)	0.1434 (4)	3.3 (3)
C(112)	0.2462 (3)	0.1857 (4)	0.1257 (4)	4.1 (3)
C(113)	0.2104 (3)	0.1199 (4)	0.1163 (4)	4.9 (4)
C(114)	0.2405 (3)	0.0503 (4)	0.1246 (4)	5.9 (4)
C(115)	0.3065 (3)	0.0465 (4)	0.1422 (4)	4.3 (3)
C(116)	0.3423 (3)	0.1123 (4)	0.1517 (4)	3.4 (3)
C(121)	0.3065 (4)	0.3442 (5)	0.1454 (3)	3.8 (3)
C(122)	0.2911 (4)	0.3894 (5)	0.2032 (3)	5.2 (4)
C(123)	0.2474 (4)	0.4485 (5)	0.1945 (3)	6.9 (4)
C(124)	0.2190 (4)	0.4625 (5)	0.1281 (3)	5.9 (4)
C(125)	0.2345 (4)	0.4174 (5)	0.0703 (3)	4.7 (3)
C(126)	0.2782 (4)	0.3582 (5)	0.0790 (3)	4.1 (3)
C(131)	0.4012 (4)	0.2687 (4)	0.0684 (4)	3.4 (3)
C(132)	0.3864 (4)	0.2172 (4)	0.0147 (4)	5.0 (4)
C(133)	0.4150 (4)	0.2242 (4)	−0.0516 (4)	6.4 (4)
C(134)	0.4583 (4)	0.2827 (4)	−0.0642 (4)	6.7 (5)
C(135)	0.4730 (4)	0.3342 (4)	−0.0106 (4)	4.9 (3)
C(136)	0.4445 (4)	0.3272 (4)	0.0558 (4)	3.9 (3)
C(211)	0.3769 (4)	0.3402 (4)	0.4169 (4)	3.3 (3)
C(212)	0.3498 (4)	0.3344 (4)	0.4840 (4)	5.1 (4)
C(213)	0.3514 (4)	0.3957 (4)	0.5300 (4)	5.2 (4)
C(214)	0.3801 (4)	0.4628 (4)	0.5089 (4)	5.1 (4)
C(215)	0.4073 (4)	0.4685 (4)	0.4418 (4)	5.2 (4)
C(216)	0.4057 (4)	0.4072 (4)	0.3958 (4)	3.9 (3)
C(221)	0.3843 (3)	0.1818 (4)	0.4162 (4)	3.2 (3)
C(222)	0.4481 (3)	0.1589 (4)	0.4300 (4)	4.6 (3)
C(223)	0.4606 (3)	0.1011 (4)	0.4781 (4)	5.8 (4)
C(224)	0.4094 (3)	0.0660 (4)	0.5125 (4)	5.7 (4)
C(225)	0.3456 (3)	0.0888 (4)	0.4987 (4)	5.1 (4)
C(226)	0.3331 (3)	0.1467 (4)	0.4505 (4)	4.4 (3)
C(231)	0.2832 (4)	0.2538 (4)	0.3391 (4)	3.8 (3)
C(232)	0.2595 (4)	0.1892 (4)	0.3059 (4)	4.1 (3)
C(233)	0.1932 (4)	0.1821 (4)	0.2910 (4)	6.4 (4)
C(234)	0.1506 (4)	0.2396 (4)	0.3092 (4)	6.8 (5)
C(235)	0.1744 (4)	0.3042 (4)	0.3423 (4)	7.2 (5)
C(236)	0.2407 (4)	0.3113 (4)	0.3573 (4)	5.0 (4)
C(1)	0.454 (2)	0.484 (2)	0.704 (3)	27 (1)*
C(2)	0.444 (2)	0.433 (3)	0.761 (2)	27 (1)*
C(3)	0.502 (2)	0.425 (2)	0.806 (2)	27 (1)*
C(4)	1.015 (3)	0.404 (2)	0.196 (2)	33 (2)*
C(5)	0.970 (3)	0.475 (3)	0.197 (3)	33 (2)*
C(6)	0.956 (3)	0.481 (3)	0.279 (3)	33 (2)*

[a] Starred values denote atoms that were refined anisotropically. Values for anisotropically refined atoms are given in the form of the equivalent isotropic displacement parameter defines as: $(4/3)[a^2\beta_{11} + b^2\beta_{22} + c^2\beta_{33} + ab(\cos\gamma)\beta_{12} + ac(\cos\beta)\beta_{13} + bc(\cos\alpha)\beta_{23}]$. [b] Atoms Re(2), P(3), and P(4) were refined with occupancies of 4%. All other atoms except for the two disordered solvent molecules (which were refined with full occupancies) were refined with occupancies of 96%. The thermal parameters for atoms C(1)–C(6) are very high, and this is reflective of the extremely disordered arrangements of these molecules. Refinement of these molecules with partial occupancies (e.g. 83%) resulted in slightly lower equivalent isotropic displacement parameters (*B*) of 21 and 30 Å² for C(1)–C(3) and C(4)–C(6), respectively.

Table IV. Positional Parameters and Their Estimated Standard Deviations for $Re_2H_8(PPh_3)_4 \cdot (CH_3)_2CO$ (**1b**)[a]

atom	x	y	z	B, Å²
Re	0.02955 (1)	0.75795 (2)	0.21633 (1)	1.793 (7)
P(1)	0.01485 (7)	0.8558 (1)	0.12907 (7)	1.92 (4)
P(2)	0.10616 (8)	0.6364 (1)	0.22706 (7)	2.16 (4)
H(1)	−0.009 (3)	0.692 (4)	0.164 (2)	5 (2)*
H(2)	0.083 (2)	0.829 (4)	0.236 (3)	3 (1)*
H(3)	0.0607 (3)	0.751 (3)	0.3066 (3)	8 (3)*
H(4)	0.000	0.6456 (5)	0.250	4 (2)*
H(5)	0.000	0.8704 (5)	0.250	8 (4)*
C(111)	0.0113 (2)	0.9936 (3)	0.1393 (1)	2.0 (2)
C(112)	−0.0208 (2)	1.0561 (3)	0.0885 (1)	2.9 (2)
C(113)	−0.0226 (2)	1.1597 (3)	0.0970 (1)	3.3 (2)
C(114)	0.0076 (2)	1.2009 (3)	0.1564 (1)	3.2 (2)
C(115)	0.0397 (2)	1.1384 (3)	0.2073 (1)	3.2 (2)
C(116)	0.0416 (2)	1.0347 (3)	0.1988 (1)	2.6 (2)
C(121)	−0.0611 (2)	0.8370 (4)	0.0609 (2)	2.3 (2)
C(122)	−0.0649 (2)	0.8233 (4)	0.0011 (2)	2.7 (2)
C(123)	−0.1234 (2)	0.8105 (4)	−0.0490 (2)	3.4 (2)
C(124)	−0.1781 (2)	0.8113 (4)	−0.0391 (2)	3.6 (2)
C(125)	−0.1743 (2)	0.8250 (4)	0.0207 (2)	4.0 (2)
C(126)	−0.1159 (2)	0.8379 (4)	0.0707 (2)	3.1 (2)
C(131)	0.0720 (2)	0.8457 (2)	0.0943 (2)	2.3 (2)
C(132)	0.0836 (2)	0.7497 (2)	0.0776 (2)	2.5 (2)
C(133)	0.1314 (2)	0.7351 (2)	0.0580 (2)	3.3 (2)
C(134)	0.1676 (2)	0.8166 (2)	0.0549 (2)	3.9 (2)
C(135)	0.1560 (2)	0.9126 (2)	0.0716 (2)	3.4 (2)
C(136)	0.1082 (2)	0.9272 (2)	0.0912 (2)	2.7 (2)
C(211)	0.0858 (2)	0.5429 (3)	0.1637 (2)	2.3 (2)
C(212)	0.1278 (2)	0.5161 (3)	0.1384 (2)	3.2 (2)
C(213)	0.1083 (2)	0.4523 (3)	0.0870 (2)	3.9 (2)
C(214)	0.0468 (2)	0.4154 (3)	0.0608 (2)	4.0 (2)
C(215)	0.0049 (2)	0.4422 (3)	0.0861 (2)	3.6 (2)
C(216)	0.0244 (2)	0.5060 (3)	0.1376 (2)	3.1 (2)
C(221)	0.1879 (2)	0.6723 (3)	0.2436 (2)	2.3 (2)
C(222)	0.1995 (2)	0.7674 (3)	0.2258 (2)	3.0 (2)
C(223)	0.2608 (2)	0.7959 (3)	0.2375 (2)	3.7 (2)
C(224)	0.3106 (2)	0.7291 (3)	0.2670 (2)	3.8 (2)
C(225)	0.2990 (2)	0.6340 (3)	0.2848 (2)	3.6 (2)
C(226)	0.2377 (2)	0.6055 (3)	0.2731 (2)	3.1 (2)
C(231)	0.1215 (2)	0.5536 (3)	0.2947 (2)	2.5 (2)
C(232)	0.1107 (2)	0.4500 (3)	0.2890 (2)	3.5 (2)
C(233)	0.1249 (2)	0.3912 (3)	0.3420 (2)	4.5 (3)
C(234)	0.1498 (2)	0.4360 (3)	0.4007 (2)	4.4 (3)
C(235)	0.1607 (2)	0.5396 (3)	0.4064 (2)	3.8 (2)
C(236)	0.1465 (2)	0.5984 (3)	0.3534 (2)	3.3 (2)
O	0.2325 (3)	0.4757 (6)	0.5563 (3)	6.6 (2)
C(1)	0.3283 (6)	0.395 (1)	0.6212 (5)	8.9 (5)
C(2)	0.2788 (4)	0.4759 (7)	0.6059 (4)	4.8 (3)
C(3)	0.2889 (5)	0.5560 (8)	0.6526 (4)	6.0 (3)

[a] Anisotropically refined atoms are given in the form of the equivalent isotropic displacement parameter defined as: $(1/3)[a^2a^{*2}B_{11} + b^2b^{*2}B_{22} + c^2c^{*2}B_{33} + 2ab(\cos\gamma)a^*b^*B_{12} + 2ac(\cos\beta)a^*c^*B_{13} + 2bc(\cos\alpha)b^*c^*B_{23}]$. Starred values denote atoms that were refined isotropically.

is no difference in the Re–Re bonding molecular orbital energies in the phosphorus-eclipsed form and the phosphorus-staggered forms of $Re_2H_8(PH_3)_4$. Furthermore, calculations for the hypothetical $Re_2H_8(PH_3)_4$ molecule showed that there was only a "tiny energy difference" between the conformations in the phosphines cis as in **1a** or trans as in **1b**.[15] Therefore, it could be that conformer **1b** is simply the result of different packing effects in the crystal containing acetone as compared to the one containing THF. The conformation present in **1b** no doubt benefits from smaller intramolecular steric interactions between adjacent phenyl groups on the PPh_3 ligand on different Re atoms.

Selected bond distances and angles are given in Table V and VI for **1a** and **1b**, respectively. The Re–Re distances in the two orientations in **1a** are equal within experimental error and have an average value of 2.53 Å. They are also equal to the Re–Re distance in $Re_2H_8(PEt_2Ph)_4$, which was determined via neutron diffraction[2] to be 2.538 (4) Å, and in $Re_2H_8(PMe_3)_4$, determined to be 2.53 Å in a preliminary X-ray structure determination.[16] The Re–Re distance in **1b**, 2.514 (0) Å, is slightly shorter.

The Re–P distances in **1a**, **1b**, and $Re_2H_8(PEt_2Ph)_4$ are all equal within experimental error. Furthermore, the PReP angles in **1a**, $Re_2H_8(PEt_2Ph)_4$, and $Re_2H_8(PMe_3)_4$ are similar, namely, 103.12 (9), 102.7 (2), and 105.4°, respectively. These angles are significantly less than the PReP angle in **1b** of 107.43 (6)°, which suggests that there may be some steric strain between PPh_3 groups on the same Re atom in the **1a** conformer.

Exchange of Bridge and Terminal Hydrogen Atoms. It has long been known that in $Re_2H_8(PPh_3)_4$ molecules generally (including the PPh_3 complex) there is rapid exchange of the bridge (H_b) and

(16) Lyons, D.; Wilkinson, G. *J. Chem. Soc., Dalton Trans.* **1985**, 587.

Table V. Selected Bond Distances and Angles for $Re_2H_8(PPh_3)_4 \cdot 2C_4H_8O$ (**1a**)[a]

Bond Distances (Å)			
Re(1)–Re(1)′	2.533 (1)	P(2)–C(211)	1.849 (8)
Re(1)–P(1)	2.357 (3)	P(2)–C(221)	1.861 (8)
Re(1)–P(2)	2.355 (3)	P(2)–C(231)	1.837 (8)
P(1)–C(111)	1.833 (7)	Re(2)–Re(2)	2.52 (2)
P(1)–C(121)	1.855 (9)	Re(2)–P(3)	2.52 (5)
P(1)–C(131)	1.862 (8)	Re(2)–P(4)	2.42 (7)

Bond Angles (deg)			
Re(1)–Re(1)–P(1)	126.96 (6)	Re(1)–P(2)–C(211)	118.4 (3)
Rel–Re(1)–P(2)	129.92 (7)	Re(1)–P(2)–C(221)	116.1 (3)
P(1)–Re(1)–P(2)	103.12 (9)	Re(1)P(2)–C(231)	118.5 (3)
Re(1)–P(1)–C(111)	118.3 (3)	C(211)–P(2)–C(221)	99.3 (4)
Re(1)–P(1)–C(121)	120.5 (3)	C(211)–P(2)–C(231)	101.5 (4)
Re(1)–P(1)–C(131)	114.6 (3)	C(221)–P(2)–C(231)	99.7 (3)
C(111)–P(1)–C(121)	103.5 (4)	Re(2)–Re(2)–P(3)	130 (1)
C(111)–P(1)–C(131)	98.6 (4)	Re(2)–Re(2)–P(4)	128 (2)
C(121)–P(1)–C(131)	97.5 (3)	P(3)–Re(2)–P(4)	103 (2)

[a] Numbers in parentheses are estimated standard deviations in the least significant digits.

Scheme I. Proposed Internal Flip of the Re–Re Bond within the Ligand Cage.

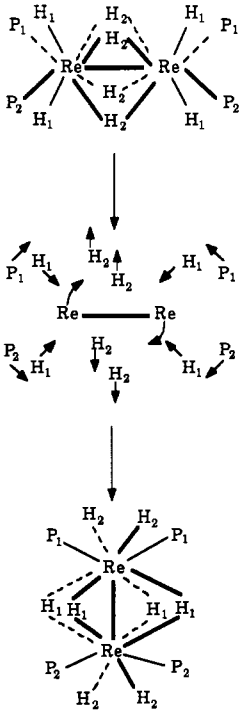

terminal (H_t) hydrogen atoms.[1,2,3b,7b] In all cases, there is only one ^1H resonance in the NMR spectrum, and this takes the form of a sharp quintet at 25 °C. The process of exchange has been shown[7b] to be very facile since temperatures of −80 °C or lower are required to observe separate signals for H_t and H_b. The NMR results for $Re_2H_8(PPh_3)_4$ are shown in Figure 1.

It is interesting to consider possible pathways for the rapid H_t/H_b exchange. In the case of the PPh_3 compound, we have explicitly ruled out any process that entails PPh_3 dissociation as the rate-determining step by showing that the ^1H NMR spectra vary with temperature in the same way whether excess PPh_3 is added to the solution or not.

Only one explicit suggestion has previously been offered.[3b] Walton and co-workers proposed a "concertina-like" process in which two H_b atoms would move to terminal positions while the P–Re–P bond angles increased to become more nearly 180°. Reversal of this process could return H_t atoms other than the H_b atoms that had just migrated to the bridging positions, and repetition of this process would allow all eight H atoms access to all eight sites. This would explain the NMR results. However, other processes may also be considered.

Table VI. Selected Atomic Distances and Angles for $Re_2H_8(PPh_3)_4 \cdot (CH_3)_2CO$ (**1b**)[a,b]

Atomic Distances (Å)			
Re–Re′	2.514 (0)	H(1)–H(2)	2.79 (7)
Re–P(1)	2.342 (2)	H(1)–H(3)	1.81 (8)
Re–P(2)	2.347 (2)	H(1)–H(4)	2.05 (6)
Re–H(1)	1.48 (5)	H(2)–H(3)	2.21 (8)
Re–H(2)	1.48 (5)	H(2)–H(5)	2.18 (6)
Re–H(3)	1.952 (7)	H(3)–H(3)′	2.978 (8)
Re–H(3)′	1.950 (8)	H(3)–H(4)	2.04 (6)
Re–H(4)	1.950 (5)	H(3)–H(5)	2.18 (6)
Re–H(5)	1.952 (5)	H(4)–H(5)	2.985 (9)
P(1)–H(1)	2.48 (6)	P(1)–C(111)	1.852 (4)
P(1)–H(2)	2.39 (5)	P(1)–C(121)	1.850 (3)
P(2)–H(1)	2.58 (6)	P(1)–C(131)	1.848 (6)
P(2)–H(2)	2.64 (5)	P(2)–C(211)	1.849 (5)
P(2)–H(3)	2.95 (4)	P(2)–C(221)	1.848 (4)
P(2)–H(4)	2.761 (2)	P(2)–C(231)	1.851 (4)

Atomic Angles (deg)			
Re–Re–P(1)	130.15 (5)	H(2)–Re–H(5)	77 (2)
Re–Re–P(2)	122.06 (5)	H(3)–Re–H(3)′	99.5 (4)
Re–Re–H(1)	103 (3)	H(3)–Re–H(4)	63 (2)
Re–Re–H(2)	115 (3)	H(3)–Re–H(5)	68 (2)
Re–Re–H(3)	49.9 (2)	H(3)′–Re–H(4)	63 (2)
Re–Re–H(3)′	49.9 (2)	H(3)′–Re–H(5)	68 (2)
Re–Re–H(4)	49.9 (1)	H(4)–Re–H(5)	99.8 (2)
Re–Re–H(5)	49.9 (1)	H(1)–P(1)–H(2)	70 (2)
P(1)–Re–P(2)	107.43 (6)	H(1)–P(2)–H(2)	65 (2)
P(1)–Re–H(1)	77 (2)	P(1)–H(1)–P(2)	97 (2)
P(1)–Re–H(2)	73 (2)	P(1)–H(2)–P(2)	97 (2)
P(1)–Re–H(3)	148 (2)	Re–H(3)–Re	80.2 (3)
P(1)–Re–H(3)′	92 (1)	H(4)–H(3)–H(5)	90.0 (3)
P(1)–Re–H(4)	147.11 (5)	Re–H(4)–Re	80.2 (3)
P(1)–Re–H(5)	89.5 (1)	H(3)–H(4)–H(3)′	94 (2)
P(2)–Re–H(1)	81 (2)	Re–H(5)–Re	80.2 (3)
P(2)–Re–H(2)	84 (2)	H(3)–H(5)–H(3)′	86 (2)
P(2)–Re–H(3)	86 (2)	Re–P(1)–C(111)	115.5 (1)
P(2)–Re–H(3)′	133 (2)	Re–P(1)–C(121)	115.3 (2)
P(2)–Re–H(4)	79.4 (1)	Re–P(1)–C(131)	119.2 (1)
P(2)–Re–H(5)	150.27 (4)	C(111)–P(1)–C(121)	99.7 (2)
H(1)–Re–H(2)	141 (4)	C(111)–P(1)–C(131)	102.2 (2)
H(1)–Re–H(3)	135 (3)	C(121)–P(1)–C(131)	102.2 (2)
H(1)–Re–H(3)′	62 (3)	Re–P(2)–C(211)	116.7 (1)
H(1)–Re–H(4)	72 (3)	Re–P(2)–C(221)	121.5 (1)
H(1)–Re–H(5)	127 (3)	Re–P(2)–C(231)	111.3 (2)
H(2)–Re–H(3)	79 (3)	C(211)–P(2)–C(231)	111.3 (2)
H(2)–Re–H(3)′	143 (3)	C(211)–P(2)–C(231)	101.2 (2)
H(2)–Re–H(4)	139 (2)	C(221)–P(2)–C(231)	99.3 (2)

[a] Numbers in parentheses are estimated standard deviations in the least significant digits. [b] The positions of the metal-bonded H atoms were optimized and refined as outlined in the Experimental Section of the paper.

For example, the less extense pattern of exchange shown in eq 1 would also account for the NMR spectra. In this process the two quasi-rectangular sets of four H atoms circulate as shown.

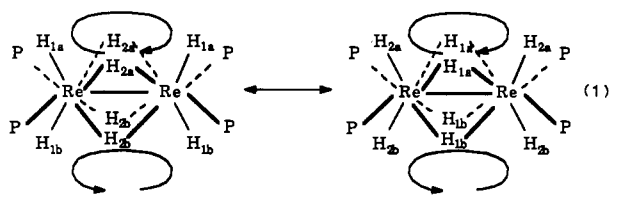

(1)

The two circulatory processes need not be correlated. In this case each H atom has access to only one subset of four sites, but the observed NMR spectra would still be explained. However, if rotation of each $Re(H_t)_2(PR_3)_2$ moiety relative to the rest of the molecule also comes into play, as suggested by the calculations mentioned above,[15] then complete scrambling over all positions would occur.

Another type of process that might occur would be coalescence of one H_t and an adjacent H_b to form an η^2-H_2 ligand, which could

rotate about the axis from Re to its midpoint. Repetition of this type of process in all the equivalent ways would give an averaged ^1H NMR spectrum. Such a mechanism would contribute to the observed short T_1(min) values found[7b] for $Re_2H_8(PR_3)_4$ molecules, but we do not believe a reverse argument (i.e., that the short T_1(min) values favor this sort of mechanism in preference to others) is persuasive.

Finally, however, we should like to propose one more mechanism, of a very different type, that is suggested by the crystallographic disorder found in **1a**. This consists of an internal flip of the Re_2 unit within the ligand cage accompanied by slight ligand rearrangements such as shown in Scheme I. Such a motion could have been responsible for creating the disorder present in **1a**. Similar internal-flip mechanisms in different complexes are now gaining general acceptance in the literature.[17]

Acknowledgment. We thank the National Science Foundation for financial support and Dr. Larry R. Falvello for his extremely helpful discussions regarding aspects of the crystallographic work.

Supplementary Material Available: Fully labeled ORTEP drawings and stereoviews of the unit cell packing for complexes **1a** and **1b**, listings of the positional parameters for the hydrogen atoms attached to phenyl rings, full tables of the crystallographic data and anisotropic displacement parameters for complexes **1a** and **1b**, and difference Fourier contour plots with all of the data and data up to (sin θ)/λ of 0.423 for complex **1b** (26 pages); listings of observed and calculated structure factors for **1a** and **1b** (49 pages). Ordering information is given on any current masthead page.

(17) (a) Cotton, F. A.; Kitagawa, S. *Polyhedron* **1988**, *7*, 463. (b) Benfield, R. E.; Braga, D.; Johnson, B. F. G. *Polyhedron* **1988**, *7*, 2549.

Contribution from the Department of Chemistry
and Molecular Structure Center, Indiana University, Bloomington, Indiana 47405

Structure and Reactivity of $ReH_4(PMe_2Ph)_4^+$

Diane M. Lunder, Mark A. Green, William E. Streib, and Kenneth G. Caulton*

Received June 7, 1989

Protonation of ReH_3P_4 (P = PMe_2Ph) with $HBF_4{\cdot}OEt_2$ in Et_2O gives $ReH_4P_4^+$, which neither exchanges with D_2 nor reacts with PhC≡CPh, CO, MeCN, or C_2H_4 under mild conditions. These results, together with an X-ray crystal structure determination, are consistent with a "classical" tetrahydride formulation for this cation, and the lack of reactivity correlates with the absence of coordinated H_2 as a ligand. NEt_3 will not deprotonate $ReH_4P_4^+$ since it is a weaker base than ReH_3P_4. The implied electron-rich character of ReH_3P_4 thus rationalizes why protonation results in formal oxidation to Re(V), rather than retention of Re(III) as in $Re(H)_2(H_2)P_4^+$. The T_1 value of the hydrogens bound to rhenium is 97 ms at −70 °C and 360 MHz.

Introduction

We have found that protonation of IrH_3P_3[1,2] and OsH_4P_3[3] (P = PMe_2Ph) with $HBF_4{\cdot}OEt_2$ gives dihydrogen complexes with the valuable feature that they participate in equilibrium dissociation of H_2 to produce the unsaturated polyhydrides $IrH_2P_3^+$ and $OsH_3P_3^+$. We were interested in whether it was possible to extend this principle to tetrakis(phosphine) complexes for the influence such increased steric hindrance could have on the resulting hydrogenation of olefins and alkynes. We report here the results of protonation of ReH_3P_4. Earlier reports[4-6] of protonation of other ReH_3L_4 species have not revealed anything about the structure or reactivity of the derived cations.

Experimental Section

Materials and Methods. All manipulations were carried out by using standard Schlenk and glove box techniques under nitrogen or vacuum. Solvents were dried over Na/K benzophenone ketyl (diethyl ether, toluene, hexane) or P_2O_5 (CH_2Cl_2). Absolute ethanol was used as received but degassed prior to use. Deuterated solvents were dried over P_2O_5 ($CDCl_3$, CD_2Cl_2) or Na/K (C_6D_6) and distilled in vacuo. Reagents were dried over P_2O_5 (CH_3CN) or CaH_2 (NEt_3) and distilled under nitrogen. Ethylene, carbon monoxide, deuterium, and diphenylacetylene were used as received. $Re(PMe_2Ph)_3Cl_3$[7] and PMe_2Ph[8] were prepared according to literature procedures.

Spectroscopy. Proton NMR spectra were recorded by using either a Nicolet EM-360 (^1H at 360 MHz) or a Bruker 500 (^1H at 500 MHz) spectrometer. Carbon NMR spectra were recorded on a Bruker 500 instrument (^{13}C at 125.7 MHz), and all were referenced to Me_4Si. Phosphorus NMR spectra were obtained on a Nicolet 360 spectrometer (^{31}P at 146 MHz) and referenced externally to 85% H_3PO_4. Proton T_1 values were determined by the inversion/recovery method at 360 MHz with a 180°–τ–90° pulse sequence. Infrared spectra were recorded as Nujol mulls by using a Perkin-Elmer 283 spectrophotomer.

Syntheses. $ReH_3(PMe_2Ph)_4$.[9] To a solution of 1.0 g (1.41 mmol) of $ReCl_3P_3$ in 50 mL of degassed absolute ethanol were added 1.0 mL (7.05 mmol) of PMe_2Ph and 1.0 g (26.5 mmol) of $NaBH_4$. The orange mixture was heated to reflux under nitrogen. After 3 h, the bright yellow suspension was cooled to room temperature and the solvent removed under vacuum. Extraction with toluene and filtration over Celite gave a yellow solution. The toluene was removed under vacuum and the resulting yellow semisolid dissolved in hot hexane. When the mixture was cooled to room temperature, golden yellow crystals of ReH_3P_4 appeared and were collected by filtration and dried under vacuum. Yield: 80%. ^1H NMR (C_6D_6): δ (ppm) −6.80 (quintet, J = 20 Hz, Re–H), 1.48 (s, P–CH_3), 7.0–7.3 (m, P–C_6H_5 (meta, para)), 7.75 (s, P–C_6H_5 (ortho)). $^{31}P\{^1H\}$ NMR (C_6D_6): δ (ppm) −19.7 (s). IR (Nujol): ν(Re–H) 1782 cm^{-1}.

$[ReH_4(PMe_2Ph)_4]BF_4$. A 60-mg sample (0.082 mmol) of ReH_3P_4 was weighed into a 100-mL Schlenk flask. A 25-mL quantity of diethyl ether was added, resulting in a yellow solution. A 10-μL portion (0.082 mmol) of $HBF_4{\cdot}OEt_2$ was added by syringe, after which the solution immediately became colorless and a white precipitate formed. After 15 min of stirring, the mixture was allowed to settle. The solvent was removed by

(1) Lundquist, E. G.; Huffman, J. C.; Folting, K.; Caulton, K. G. *Angew. Chem., Int. Ed. Engl.* **1988**, *27*, 1165.
(2) Marinelli, G.; Rachidi, I. E.-I.; Streib, W. E.; Eisenstein, O.; Caulton, K. G. *J. Am. Chem. Soc.* **1989**, *111*, 2346.
(3) Johnson, T. J.; Huffman, J. C.; Caulton, K. G.; Jackson, S. A.; Eisenstein, O. *J. Am. Chem. Soc.*, submitted for publication.
(4) Freni, M.; Demichelis, R.; Giusto, D. *J. Inorg. Nucl. Chem.* **1967**, *29*, 1433.
(5) Chiu, K. W.; Howard, C. G.; Rzepa, H. S.; Sheppard, R. N.; Wilkinson, G. *Polyhedron* **1982**, *1*, 441.
(6) Moehring, G. A.; Walton, R. A. *Inorg. Chem.* **1987**, *26*, 2910.
(7) Douglas, P. G.; Shaw, B. L. *Inorg. Synth.* **1977**, *17*, 65.
(8) Adams, R.; Raynor, J. *Advanced Practical Inorganic Chemistry*; J. Wiley: New York, 1965.
(9) Roberts, D. A.; Geoffroy, G. L. *J. Organomet. Chem.* **1981**, *214*, 221.

0020-1669/89/1328-4527$01.50/0